·Basic Research·

Acellular ostrich corneal stroma used as scaffold for construction of tissue-engineered cornea

Xian-Ning Liu[1,2,3], Xiu-Ping Zhu[1,2,3], Jie Wu[3], Zheng-Jie Wu[4], Yong Yin[1,2,3], Xiang-Hua Xiao[1,2,3], Xin Su[4], Bin Kong[4], Shi-Yin Pan[1,2,3], Hua Yang[1,2,3], Yan Cheng[3], Na An[1,2,3], Sheng-Li Mi[4]

[1]Shaanxi Institute of Ophthalmology, Xi'an 710002, Shaanxi Province, China
[2]Shaanxi Key Laboratory of Eye, Xi'an 710002, Shaanxi Province, China
[3]Xi'an First Hospital, Xi'an 710002, Shaanxi Province, China
[4]Biomanufacturing Engineering Laboratory, Graduate School at Shenzhen, Tsinghua University, Shenzhen 518055, Guangdong Province, China

Correspondence to: Sheng-Li Mi. Biomanufacturing Engineering Laboratory, Graduate School at Shenzhen, Tsinghua University, Shenzhen 518055, Guangdong Province, China. mi.shengli@sz.tsinghua.edu.cn
Received: 2015-06-19 Accepted:2016-02-15

Abstract

• AIM: To assess acellular ostrich corneal matrix used as a scaffold to reconstruct a damaged cornea.

• METHODS: A hypertonic saline solution combined with a digestion method was used to decellularize the ostrich cornea. The microstructure of the acellular corneal matrix was observed by transmission electron microscopy (TEM) and hematoxylin and eosin (H&E) staining. The mechanical properties were detected by a rheometer and a tension machine. The acellular corneal matrix was also transplanted into a rabbit cornea and cytokeratin 3 was used to check the immune phenotype.

• RESULTS: The microstructure and mechanical properties of the ostrich cornea were well preserved after the decellularization process. *In vitro*, the methyl thiazolyl tetrazolium results revealed that extracts of the acellular ostrich corneas (AOCs) had no inhibitory effects on the proliferation of the corneal epithelial or endothelial cells or on the keratocytes. The rabbit lamellar keratoplasty showed that the transplanted AOCs were transparent and completely incorporated into the host cornea while corneal turbidity and graft dissolution occurred in the acellular porcine cornea (APC) transplantation. The phenotype of the reconstructed cornea was similar to a normal rabbit cornea with a high expression of cytokeratin 3 in the superficial epithelial cell layer.

• CONCLUSION: We first used AOCs as scaffolds to reconstruct damaged corneas. Compared with porcine corneas, the anatomical structures of ostrich corneas are closer to those of human corneas. In accordance with the principle that structure determines function, a xenograft lamellar keratoplasty also confirmed that the AOC transplantation generated a superior outcome compared to that of the APC graft.

• **KEYWORDS:** ostrich; acellular corneal stroma; tissue engineering; cornea

DOI:10.18240/ijo.2016.03.01

Liu XN, Zhu XP, Wu J, Wu ZJ, Yin Y, Xiao XH, Su X, Kong B, Pan SY, Yang H, Cheng Y, An N, Mi SL. Acellular ostrich corneal stroma used as scaffold for construction of tissue-engineered cornea. *Int J Ophthalmol* 2016;9(3):325-331

INTRODUCTION

Corneal transplantation is presently the only effective method for the visual rehabilitation of patients with corneal blindness. However, there is an increasing need for human donor corneal tissue and a shortage of suitable cornea donors. Therefore, many researchers have attempted to fabricate alternatives to donor corneas for the treatment of corneal blindness[1-4].

Recently, new scaffolds for tissue engineering based on native tissues have become an attractive option. The primary objectives of preparing a decellularized extracellular matrix (ECM) are to eliminate tissue immunogenicity and retain the three-dimensional spatial structure of the ECM of native tissues[5]. Acellular porcine corneas (APCs) are composed of natural stromal proteins that exhibit reasonable structural characteristics. Several research groups have succeeded in preparing a porcine acellular corneal stroma using detergent and/or several enzymes[6-11].

The five largest eyes in the vertebrate kingdom are those of the whale, elephant, zebra, giraffe and ostrich. The axial length of the eye in these species ranges from 54 mm in the baleen whale to 39 mm in the ostrich [12]. The ostrich cornea is large enough to be trimmed to fit the human eye and ostrich corneas are an abundant resource. The goal of this study was to use an acellular ostrich cornea (AOC) stroma to replace an APC as a new scaffold to construct a tissue-engineered cornea (TEC). We hope that the AOCs will prove to be a potential solution to the short supply of donor corneas.

MATERIALS AND METHODS

Animals Whole ostrich eyes (either gender, 12 months old, weighing 60-70 kg) and Yorkshire Landrace pig eyes (either gender, 6 months old, weighing 120-150 kg) were obtained within 1-3h of postmortem and subjected to a decellularization procedure within 2h of receipt. The native ostrich corneas/porcine corneas with 2 mm scleral rings were removed with a pair of curved scissors. Young adult New Zealand white rabbits (either gender, 10 weeks old, weighing 2-3 kg) were used as animal transplant models. All animal experiments conformed to the Association for Research in Vision and Ophthalmology statement for the use of animals in ophthalmic and vision research.

Preparation of Acellular Ostrich Corneas The above corneoscleral tissues were rinsed three times with phosphate buffered saline (PBS). Then, a lamellar cornea stroma with a diameter of 12 mm ring and thickness of 400 microns was acquired by scaled trephine under an ophthalmologic microscope (Olympus, Japan). Subsequently, the lamellar cornea was soaked in hypertonic saline solution with 20% NaCl (w/v) for 48h at 37℃. Next, the corneal grafts were immersed in 0.13% trypsin solution (GIBCO,USA) or trypLE™ Express (1×) solution (GIBCO) for 48h at 37℃ and then washed in ultrapure water 3 times for 30min each time. Finally, the grafts were put into a sealed dry container and dehydrated with calcium chloride for 1-2d at room temperature. The prepared AOCs were sealed in sterile plastic envelopes, sterilized by g-irradiation (25 kGy) and stored at 4℃ until used.

Hematoxylin and Eosin Staining Native corneas (ostrich, human and porcine) and transplanted corneas were collected and examined with hematoxylin and eosin (H&E) staining. The tissues were wax-embedded, processed routinely and examined using light microscopy after H&E staining.

Transmission Electron Microscopy Native ostrich, human and porcine corneas were collected and examined with transmission electron microscopy (TEM). Specimens were fixed in 2.5% glutaraldehyde in PBS, washed three times in PBS for 15min each time, and post-fixed for 2h in 2% aqueous osmium tetroxide. They were washed three more times in PBS before being passed through a graded ethanol series. For the purposes of TEM, the specimens were embedded in an epoxy resin (Agar Scientific, Ltd., Stansted, UK). Ultrathin (70 nm) sections were collected on copper grids and stained for 1h with uranyl acetate and 1% phosphotungstic acid and then for 20min with Reynolds' lead citrate before being examined with a transmission electron microscope (Philips CM10).

Rheology Measurements of the rheological properties were carried out for natural ostrich corneas (n=5) and AOCs (n=5). A controlled shear stress rheometer (Anton Paar, MCR302, Austria) was used for the measurement. The real part of the rigidity modulus, G' is the elastic or storage modulus and its imaginary part, G'' is the viscous or loss modulus. Two types of oscillatory measurements were performed: 1)frequency oscillatory measurement: a declining frequency from 100 to 0.1 Hz was applied on the rotation. As the applied frequency declines, the stress increases; 2) strain oscillatory measurement: a sinusoidal strain from 0.01 to 100 Hz was applied on the rotation. As the applied strain increases, the stress increases.

Assessment of Mechanical Properties of Different Grafts According to a previously reported method[13], the maximum static tension was measured using an Instron electromechanical universal tester (Instron, UK) equipped with Bluehill 2.35 software (n=8). The specimens were kept wet using PBS and cut into 10×4 mm^2 rectangular strips. The load range was set to 0-100 mol/L, and the crosshead speed was 0.3 mm/min. Native ostrich corneas were used as a control (n=8).

Cytotoxicity of Extractable Materials To determine whether extracts from the AOCs would cause cytotoxicity, each scaffold (10 mm diameter) was extracted using a 5 mL 1:1 mixture of Dulbecco's minimal essential medium and Ham's F12 medium containing 10% fetal bovine serum (culture medium) at 37℃ for 48h. Primary rabbit corneal keratocytes (1×10^3), epithelial (2×10^3) and endothelial (2×10^3) cells were separately seeded into each well of 96-well plates then cultured with extracts (the experimental group, n=5) and above culture medium (control group, n=5). The proliferation activity of the cells was quantitatively determined at 1, 3, 5, and 7d by an MTT assay. The optical density (OD) value of the absorbance at 490 nm was measured with a microplate reader (Rayto, RT2100). The differences in the OD values between the experimental and control groups were subjected to statistical analysis.

Xenograft Lamellar Keratoplasty Lamellar keratoplasty was used to evaluate the therapeutic effects. To perform lamellar keratoplasty, a circular incision with a depth of approximately 300 mm was made in the right eye. The anterior lamellar stroma was then dissected using a fine operating knife. AOCs were fixed into the recipient bed with interrupted 10-0 sutures. The control group of five rabbits was implanted with APCs.

Immunofluorescence For histological analysis, the corneas were harvested from the transplanted rabbits and examined by immunofluorescence. Prior to immunocytochemistry, each section (5 μm thick) was incubated overnight at 4℃ with primary antibodies against Cytokeratin 3 (CK3, 1:50; Millipore). Fluorescein isothiocyanate (FITC)-labeled secondary antibodies (1:50; Sigma) were used for 1h at room temperature. Sections were co-stained with 4',6-diamidino-2-phenylindole (DAPI, Sigma) and observed by fluorescence confocal microscopy (Xcellence-DSU, Olympus, Japan).

Table 1 The comparison of anatomical considerations of the cornea

Contents	Ostrich (n=10)	Human (n=10)	Porcine (n=10)
Cell layers of central corneal epithelium	4-6	5	7-9
The full thickness of central cornea (μm)	550±35	525±25	689±68
Refractive power (Diopter)	44.1	43.0	40.3
The axial length of eye (mm)	38.7	23.7	21.7

Comparing the corneal anatomical structure of ostrich, human and porcine, the ostrich is closer to human.

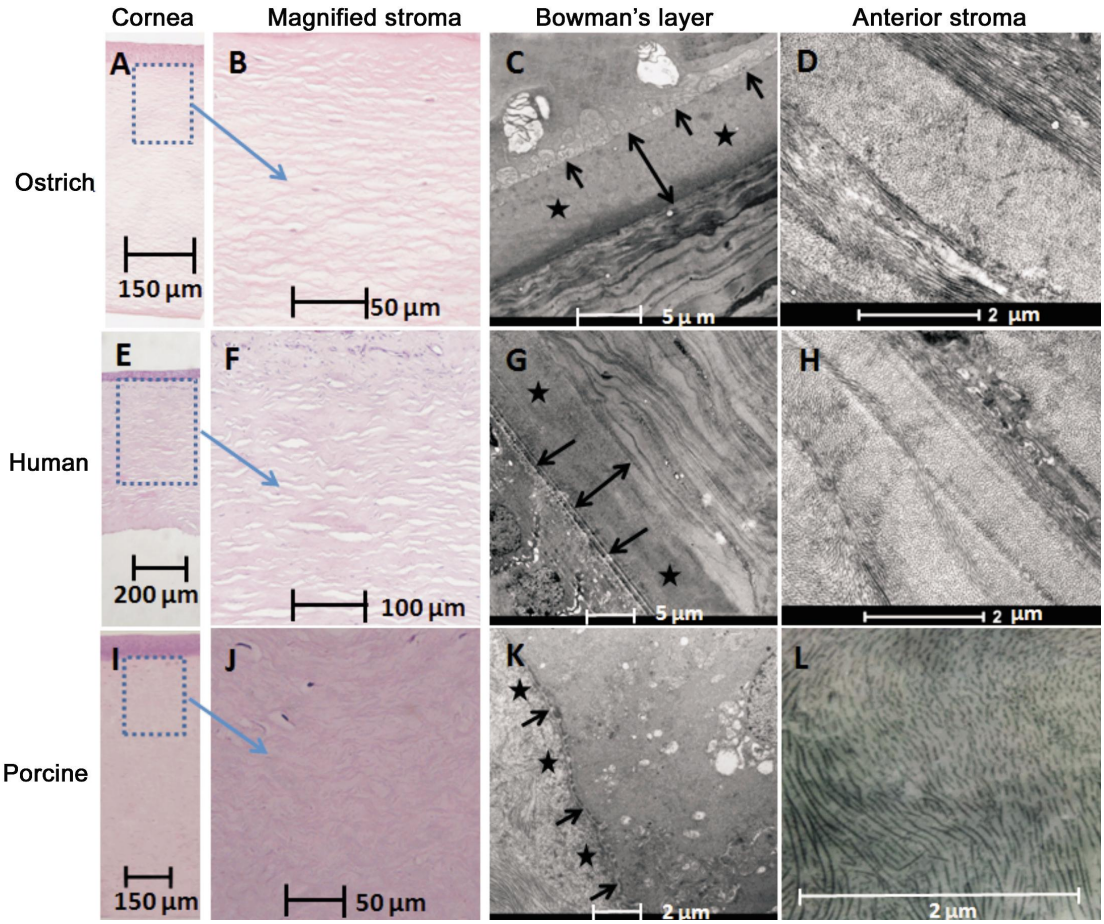

Figure 1 The histological structure examination Ostrich cornea (A and B is H&E staining, C and D is TEM); human cornea (E and F is H&E staining, G and H is TEM); porcine cornea (I and J is H&E staining, K and L is TEM).

Statistical Analysis All data are expressed as the mean±SD. A Student's t-test (unpaired) was performed with Microsoft Excel to analyze the data. The results are presented as the mean of three individual experiments with the standard error of the mean and a P-value less than 0.05 was considered significant.

RESULTS

Anatomical Structure of the Cornea Comparison of the corneal anatomical structure of the ostrich (cell layers of the central epithelium, the thickness of the central cornea, refractive power) to that of a human or pig showed that the ostrich cornea is most similar to that of the human. Another advantage is that the ostrich corneal area is larger and is more readily available (Table 1).

Histological Structure of the Acellular Corneal Stroma and Natural Human Cornea The histological structure examination showed that all the corneas had similar lamellar structures. The thickness of the ostrich cornea was closest to that of a human (Figure 1A, 1E), and the thickest was the porcine cornea (Figure 1I). The ostrich and human corneas had well-developed anterior corneal elastic layers (Figure 1C, 1G, indicated with asterisks, its thickness shown with double arrows) and base membranes (single arrows). The anterior corneal elastic layer of porcine corneas was hypogenic (Figure 1K, shown by asterisks, its thickness was very thin), while the base membrane was completely developed (single arrows). Corneal stromal collagen fibers of ostrich and human corneas were arranged regularly and formed oriented lamellar structures (Figure 1D, 1H). The anterior collagen fibers of the porcine corneal stroma were disordered (Figure 1L), while the posterior collagen fibers were relatively ordered.

Preparation of the Acellular Ostrich Corneas and Histological Examination The AOCs were decellularized

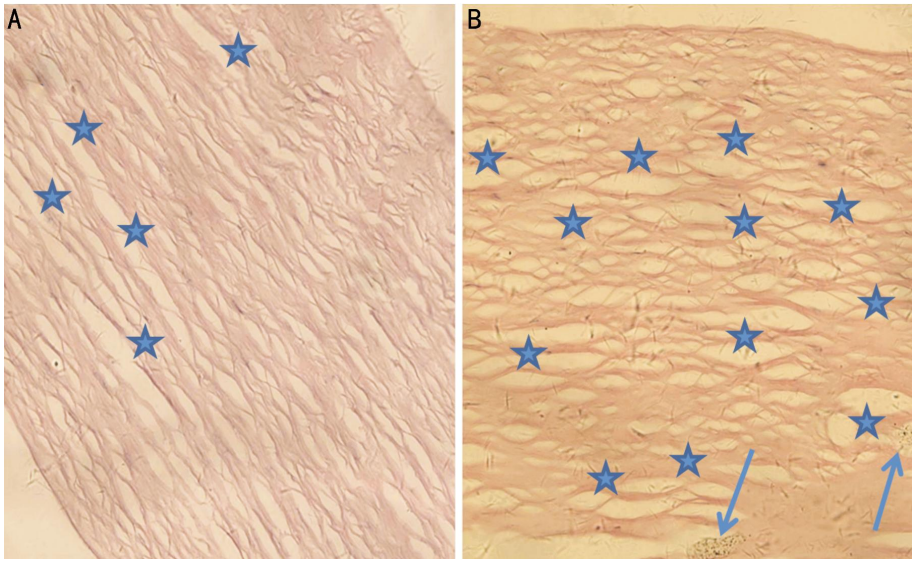

Figure 2 The H&E staining of AOCs after trypLE™ Express digestion (A) and trypsin digestion (B) Magnification ×400.

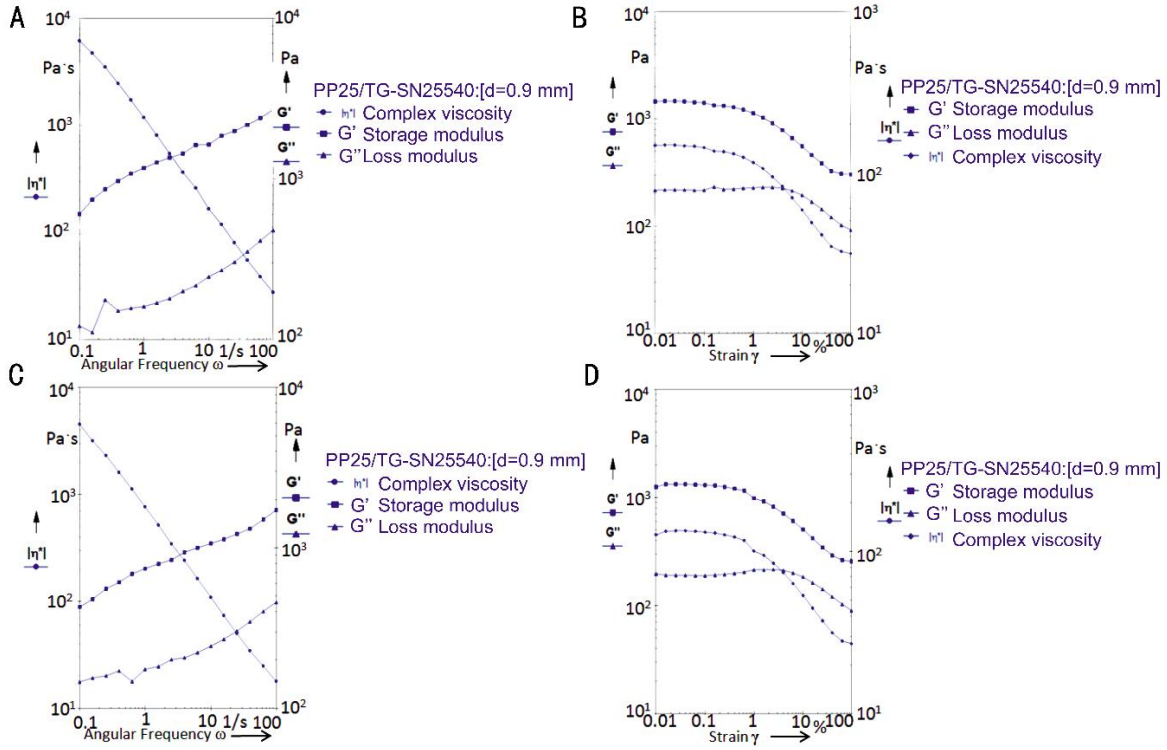

Figure 3 The rheology test of the natural ostrich cornea (A&B) and AOCs (C&D) Fixed amplitude and frequency swing (A&C), fixed frequency and amplitude swing (B&D). The rheology results of the scaffolds revealed that there were no significant differences before and after decellularization.

using a hypertonic saline solution combined with an enzyme/trypLE™ Express digestion method. The H&E staining showed that the gaps between the collagen fibers after trypsin digestion (Figure 2B, denoted by the star symbol) were larger than the gaps when digested by trypLE™ Express (Figure 2A, shown by stars). The trypsin-digested scaffolds also retained much more cell debris (Figure 2B, shown with single arrows) compared to the trypLE™ Express-digested group (Figure 2A).

Rheology The represented the storage modulus, which characterized the elastic property of the scaffolds. The is the loss modulus, which characterized the viscosity of the scaffolds. The rheology results of the scaffolds revealed that there were no significant differences before and after decellularization. Representative experimental results were shown in Figure 3.

Assessment of Mechanical Properties of the Different Grafts The maximum static tension of the natural ostrich corneal grafts was 14.1±2.3 mol/L (n=8), and the maximum static tension of the ostrich acellular grafts was 13.9±2.5 mol/L (n=8). There was no significant difference between these two groups (P>0.05). Representative experimental results are shown in Figure 4.

Cytotoxicity of Extractable Materials There were no

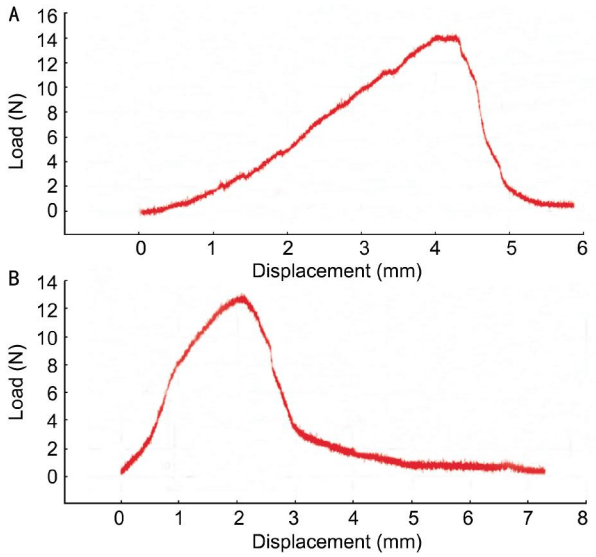

Figure 4 The typical experimental results of the maximum static tension of natural ostrich corneas (A) and the AOCs (B).

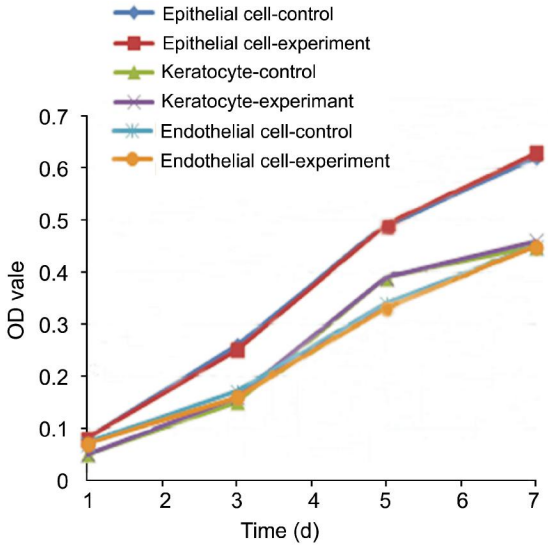

Figure 5 The effect of AOC extracts on the proliferation of corneal cells.

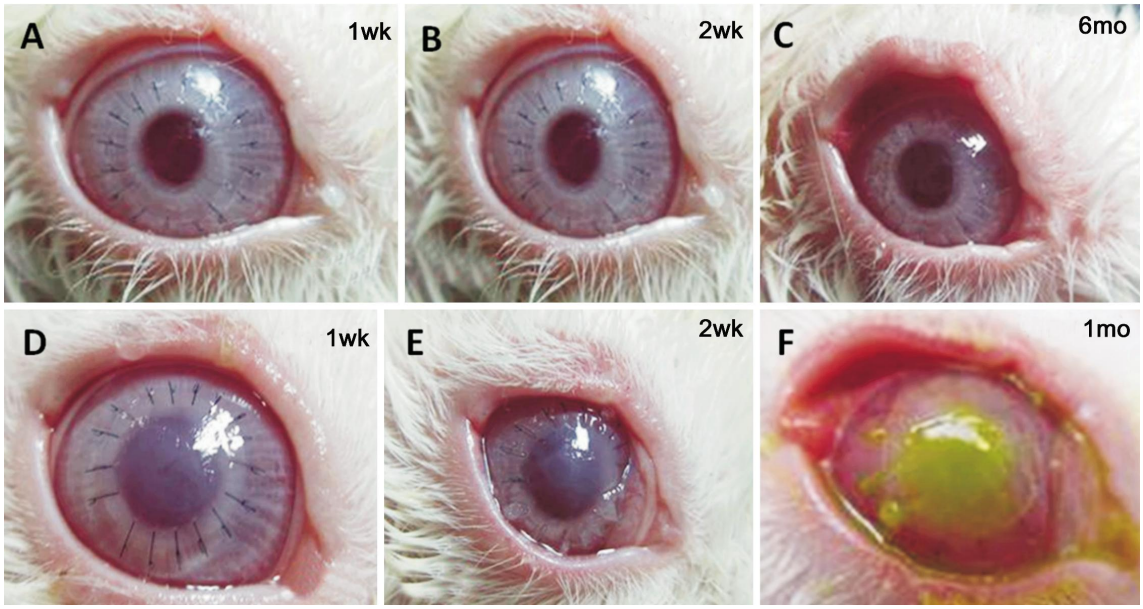

Figure 6 Representative images of the process of the restoration of transparency after transplantation The AOCs transplantation group (A-C) and APCs transplantation group (D-F). Six months following the ostrich lamellar keratoplasty, the graft remains completely transparent (C). Seven to fourteen days following the porcine lamellar keratoplasty, corneal turbidity occurred in a few cases (D, E). After 30d, some grafts began to dissolve which was revealed by fluorescein staining (F).

significant differences in the proliferation of rabbit corneal epithelial and endothelial cells or keratocytes between the experimental and control groups as determined by MTT assay (n=5, P>0.05) (Figure 5).

Xenograft Lamellar Keratoplasty Six months after the ostrich lamellar keratoplasty, the grafts remained completely transparent, they did not dissolve and there were no obvious immune rejection reactions, infections, interlayer hematoceles, interlamellar dropsies or broken line situations (Figure 6C). Seven to fourteen days following the porcine lamellar keratoplasty, corneal turbidity occurred in a few cases (Figure 6D, 6E). After 30d, some grafts began to dissolve, which was revealed by fluorescein staining (Figure 6F).

Immunofluorescence Cytokeratin 3 (CK3), often used as a specific marker in corneal epithelial cells, was highly expressed in the superficial epithelial cells but was not found in the basal epithelial cells (Figure 7C). This type of CK3 expression pattern is similar to the normal corneal immune phenotype.

DISCUSSION

Recently, there have been many reports on acellular porcine corneal grafts [6-11,14-19]. Compared with porcine eyes, the ostrich eye is larger and has better eyesight. More importantly, the anatomical structures and the diopter of ostrich eyes are closer to those of human eyes (Table 1, Figure 1). Firstly, the basic structure of corneas is a lamellar structure but the porcine cornea is thicker and has more epithelial cell layers and the thickness and epithelial cell

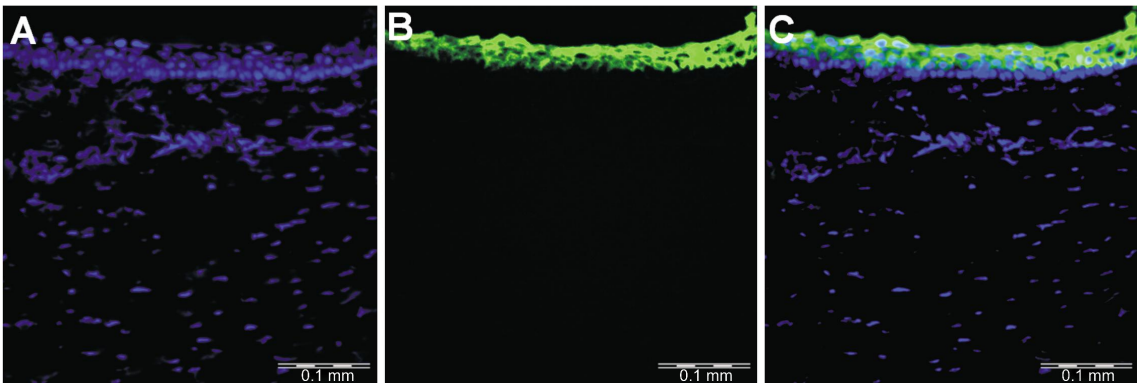

Figure 7 Immunofluorescent staining and laser scanning confocal microscopy of a corneal epithelium A: 4',6-diamidino-2-phenylindole stained the nucleus; B: CK3 stained the cytoplasm; C: The merged color image. CK3 was highly expressed in the superficial epithelial cells but was not found in the basal epithelial cells. This type of CK3 expression pattern is similar to the normal corneal immune phenotype.

layers of ostrich corneas are closer to those of human corneas. Secondly, the porcine corneal Bowman's layer structure is dysplastic, while both the ostrich and human corneas have fully developed Bowman's layers (Figure 1). The Bowman's layer may play a role in maintaining the corneal surface shape and structural stability [20]. Thirdly, the human and ostrich anterior corneal collagen fibers are regularly arranged but the porcine collagen fibers of the anterior corneal stroma are irregularly arranged. The orientation degree of the corneal collagen fibers is positively correlated to the corneal transparency [21-23] and the lamellar corneal transplantation mainly uses the anterior corneal stroma. Using the principle that structure determines function, the potential application prospects of ostrich acellular corneal scaffolds in tissue-engineered corneas are better than those of porcine acellular corneal scaffolds.

Corneal transplant surgeries also revealed that the mechanical properties of APCs became weak after rehydration; in some cases, the APCs were unable to tolerate the suture operation. Even after transplantation, the cornea initially retained transparency but approximately 10d after the operation, corneal turbidity occurred and after 30d, part of the scaffold had dissolved (Figure 6). In contrast with the rehydrated APCs, the rehydration of AOCs acquired a high transparency and there was no significant difference in the mechanical properties (elasticity, viscosity and maximum static tension) before and after decellularization (Figures 3, 4). The rehydrated AOCs were able to withstand the suture operation. Six months after the operation, the cornea maintained complete transparency and integrity (neither neovascularization nor degradation was observed), suggesting a very low immunogenicity (Figure 6).

In previous studies, many proteases and chemical reagents (trypsin, dispase, sodium dodecyl sulfate and sodium hydroxide)[6-8,15] were used to decellularize the corneal cells. Although the corneal cells were removed completely and good biocompatibility was observed [14], the decellularization reagents inevitably altered the extracellular matrix (ECM) composition (the process may remove laminin, fibronectin and glycosaminoglycans [5] and cause a certain degree of ultra-structural disruption)[15]. In this study, we used a gentle decellularization method (hypertonic saline solution combined with trypLE™ Express digestion) to prepare the acellular corneal scaffolds. This study chose trypLE™ Express to replace traditional trypsin because 1) trypLE™ Express is non-animal-derived and of a high purity and the degradation of the ECM is minimal. Trypsin is derived from animals, thus, there are differences between batches and the collapsing force of the ECM is strong; 2) trypLE™ Express is mild and does not require an enzyme inhibitor; 3) the digestion kinetics and shear specificity between trypsin and trypLE™ Express are similar but the stability of the latter is significantly higher than that of the former. Trypsin-treated scaffolds easily incur differences between batches.

ACKNOWLEDGEMENTS

Foundations: Supported by National Natural Science Foundation of China (No. 31200724); Key Innovation Project of Shaanxi Science and Technology Plan (No. 2012KTCQ03-11); Shenzhen Peacock Plan (No. KQCX20130628155525051); Projects of Basic Research of Shenzhen (No. JCYJ20120614193611639, No. JCYJ 20140509172959988).

Conflicts of Interest: Liu XN, None; **Zhu XP,** None; **Wu J,** None; **Wu ZJ,** None; **Yin Y,** None; **Xiao XH,** None; **Su X,** None; **Kong B,** None; **Pan SY,** None; **Yang H,** None; **Cheng Y,** None; **An N,** None; **Mi SL,** None.

REFERENCES

1 Levis HJ, Kureshi AK, Massie I, Morgan L, Vernon AJ, Daniels JT. Tissue engineering the cornea: the evolution of RAFT. *J Funct Biomater* 2015;6(1):50-65.

2 Harkin DG, George KA, Madden PW, Schwab IR, Hutmacher DW, Chirila TV. Silk fibroin in ocular tissue reconstruction. *Biomaterials* 2011; 32(10):2445-2458.

3 Mi S, Chen B, Wright B, Connon CJ. Ex vivo construction of an artificial ocular surface by combination of corneal limbal epithelial cells and a compressed collagen scaffold containing keratocytes. *Tissue Eng Part A* 2010;16(6): 2091-2100.

4 Feng Y, Foster J, Mi S, Chen B, Connon C. Influence of substrate on corneal epithelial cell viability within ocular surface models. *Exp Eye Res* 2012;101:97-103.

5 Sanchez PL, Fernandez-Santos ME, Costanza S, *et al* Acellular human heart matrix: A critical step toward whole heart grafts. *Biomaterials* 2015; 61:279-289.

6 Wu Z, Zhou Y, Li N, Huang M, Duan H, Ge J, Xiang P, Wang Z. The use of phospholipase A2 to prepare acellular porcine corneal stroma as a tissue engineering scaffold. *Biomaterials* 2009;30(21):3513-3522.

7 Hashimoto Y, Funamoto S, Sasaki S, Honda T, Hattori S, Nam K, Kimura T, Mochizuki M, Fujisato T, Kobayashi H, Kishida A. Preparation and characterization of decellularized cornea using high-hydrostatic pressurization for corneal tissue engineering. *Biomaterials* 2010;31 (14): 3941-3948.

8 Pang K, Du L, Wu X. A rabbit anterior cornea replacement derived from acellular porcine cornea matrix, epithelial cells and keratocytes. *Biomaterials* 2010;31(28):7257-7265.

9 Lynch AP, Ahearne M. Strategies for developing decellularized corneal scaffolds. *Exp Eye Res* 2013;108:42-7.

10 Diao JM, Pang X, Qiu Y, Miao Y, Yu MM, Fan TJ. Construction of a human corneal stromal equivalent with non-transfected human corneal stromal cells andacellular porcine corneal stromata. *Exp Eye Res* 2015; 132:216-224.

11 Xu YG, Xu YS, Huang C, Feng Y, Li Y, Wang W. Development of a rabbit corneal equivalent using an acellular corneal matrix of a porcine substrate. *Mol Vis* 2008;14:2180-2189.

12 Kiladze AB. Structural organization of anterior corneal epithelium of the African ostrich eye. *Morfologiia* 2013;143(1):32-36.

13 Mi S, Dooley EP, Albon J, Boulton ME, Meek KM, Kamma-Lorger CS. Adhesion of laser in situ keratomileusis-like flaps in the cornea: Effects of crosslinking, stromal fibroblasts, and cytokine treatment. *J Cataract Refract Surg* 2011;37(1):166-172.

14 Luo H, Lu Y, Wu T, Zhang M, Zhang Y, Jin Y. Construction of tissue engineered cornea composed of amniotic epithelial cells and acellularporcine cornea for treating corneal alkali burn. *Biomaterials* 2013; 34 (28):6748-6759.

15 Zhu J, Zhang K, Sun Y, Gao X, Li Y, Chen Z, Wu X. Reconstruction of functional ocular surface by acellular porcine cornea matrix scaffold and limbal stem cells derived from human embryonic stem cells. *Tissue Eng Part A* 2013;19(21-22):2412-2425.

16 Huang M, Li N, Wu Z, Wan P, Liang X, Zhang W, Wang X, Li C, Xiao J, Zhou Q, Liu Z, Wang Z. Using acellular porcine limbal stroma for rabbit limbal stem cell microenvironment reconstruction. *Biomaterials* 2011;32 (31):7812-7821.

17 Xiao J, Duan H, Liu Z, Wu Z, Lan Y, Zhang W, Li C, Chen F, Zhou Q, Wang X, Huang J, Wang Z. Construction of the recellularized corneal stroma using porous acellular corneal scaffold. *Biomaterials* 2011; 32(29): 6962-6971.

18 Zhang MC, Liu X, Jin Y, Jiang DL, Wei XS, Xie HT. Lamellar keratoplasty treatment of fungal corneal ulcers with acellular porcine corneal stroma. *Am J Transplant* 2015;15(4):1068-1075.

19 Shao Y, Yu Y, Pei CG, Zhou Q, Liu QP, Tan G, Li JM, Gao GP, Yang L. Evaluation of novel decellularizing corneal stroma for cornea tissue engineering applications. *Int J Ophthalmol* 2012;5(4):415-418.

20 Wang Q, Li W. Advancement of Bowmanps membrane of cornea. *Int J Ophthalmol* 2009;9 (12):2353-2356.

21 Chen S, Mienaltowski MJ, Birk DE. Regulation of corneal stroma extracellular matrix assembly. *Exp Eye Res* 2015;133:69-80.

22 Hassell JR, Birk DE. The molecular basis of corneal transparency. *Exp Eye Res* 2010;91(3):326-335.

23 Qazi Y, Wong G, Monson B, Stringham J, Ambati BK. Corneal transparency: genesis, maintenance and dysfunction. *Brain Res Bull* 2010; 81(2-3):198-210.